Inclusive cross section and double-helicity asymmetry for π^0 production at midrapidity in $p+p$ collisions at $\sqrt{s} = 510$ GeV

A. Adare,[13] C. Aidala,[38, 42] N.N. Ajitanand,[60] Y. Akiba,[55, 56] R. Akimoto,[12] J. Alexander,[60] M. Alfred,[22] K. Aoki,[31, 55] N. Apadula,[27, 61] Y. Aramaki,[55] H. Asano,[34, 55] E.T. Atomssa,[61] T.C. Awes,[51] B. Azmoun,[7] V. Babintsev,[23] M. Bai,[6] X. Bai,[11] N.S. Bandara,[41] B. Bannier,[61] K.N. Barish,[8] S. Bathe,[5, 56] V. Baublis,[54] C. Baumann,[7] S. Baumgart,[55] A. Bazilevsky,[7] M. Beaumier,[8] S. Beckman,[13] R. Belmont,[13, 42, 65] A. Berdnikov,[58] Y. Berdnikov,[58] D. Black,[8] D.S. Blau,[33] J.S. Bok,[49] K. Boyle,[56] M.L. Brooks,[38] J. Bryslawskyj,[5] H. Buesching,[7] V. Bumazhnov,[23] S. Butsyk,[48] S. Campbell,[14, 27] C.-H. Chen,[56] C.Y. Chi,[14] M. Chiu,[7] I.J. Choi,[24] J.B. Choi,[10] S. Choi,[59] P. Christiansen,[39] T. Chujo,[64] V. Cianciolo,[51] Z. Citron,[66] B.A. Cole,[14] N. Cronin,[43, 61] N. Crossette,[43] M. Csanád,[16] T. Csörgő,[67] D. Danley,[50] A. Datta,[48] M.S. Daugherity,[1] G. David,[7] K. DeBlasio,[48] K. Dehmelt,[61] A. Denisov,[23] A. Deshpande,[56, 61] E.J. Desmond,[7] L. Ding,[27] A. Dion,[61] P.B. Diss,[40] J.H. Do,[68] L. D'Orazio,[40] O. Drapier,[35] A. Drees,[61] K.A. Drees,[6] J.M. Durham,[38] A. Durum,[23] T. Engelmore,[14] A. Enokizono,[55, 57] H. En'yo,[55, 56] S. Esumi,[64] K.O. Eyser,[7] B. Fadem,[43] N. Feege,[61] D.E. Fields,[48] M. Finger,[9] M. Finger, Jr.,[9] F. Fleuret,[35] S.L. Fokin,[33] J.E. Frantz,[50] A. Franz,[7] A.D. Frawley,[18] Y. Fukao,[31] T. Fusayasu,[45] K. Gainey,[1] C. Gal,[61] P. Gallus,[15] P. Garg,[3] A. Garishvili,[62] I. Garishvili,[37] H. Ge,[61] F. Giordano,[24] A. Glenn,[37] X. Gong,[60] M. Gonin,[35] Y. Goto,[55, 56] R. Granier de Cassagnac,[35] N. Grau,[2] S.V. Greene,[65] M. Grosse Perdekamp,[24] Y. Gu,[60] T. Gunji,[12] H. Guragain,[19] T. Hachiya,[55] J.S. Haggerty,[7] K.I. Hahn,[17] H. Hamagaki,[12] H.F. Hamilton,[1] S.Y. Han,[17] J. Hanks,[61] S. Hasegawa,[28] T.O.S. Haseler,[19] K. Hashimoto,[55, 57] R. Hayano,[12] X. He,[19] T.K. Hemmick,[61] T. Hester,[8] J.C. Hill,[27] R.S. Hollis,[8] K. Homma,[21] B. Hong,[32] T. Hoshino,[21] N. Hotvedt,[27] J. Huang,[7, 38] S. Huang,[65] T. Ichihara,[55, 56] Y. Ikeda,[55] K. Imai,[28] Y. Imazu,[55] M. Inaba,[64] A. Iordanova,[8] D. Isenhower,[1] A. Isinhue,[43] D. Ivanishchev,[54] B.V. Jacak,[61] S.J. Jeon,[44] M. Jezghani,[19] J. Jia,[7, 60] X. Jiang,[38] B.M. Johnson,[7] E. Joo,[32] K.S. Joo,[44] D. Jouan,[52] D.S. Jumper,[24] J. Kamin,[61] S. Kanda,[12, 31, 55] B.H. Kang,[20] J.H. Kang,[68] J.S. Kang,[20] J. Kapustinsky,[38] D. Kawall,[41] A.V. Kazantsev,[33] J.A. Key,[48] V. Khachatryan,[61] P.K. Khandai,[3] A. Khanzadeev,[54] K. Kihara,[64] K.M. Kijima,[21] C. Kim,[32] D.H. Kim,[17] D.J. Kim,[29] E.-J. Kim,[10] G.W. Kim,[17] H.-J. Kim,[68] M. Kim,[59] Y.-J. Kim,[24] Y.K. Kim,[20] B. Kimelman,[43] E. Kistenev,[7] R. Kitamura,[12] J. Klatsky,[18] D. Kleinjan,[8] P. Kline,[61] T. Koblesky,[13] M. Kofarago,[16] B. Komkov,[54] J. Koster,[56] D. Kotchetkov,[50] D. Kotov,[54, 58] F. Krizek,[29] K. Kurita,[57] M. Kurosawa,[55, 56] Y. Kwon,[68] R. Lacey,[60] Y.S. Lai,[14] J.G. Lajoie,[27] A. Lebedev,[27] D.M. Lee,[38] G.H. Lee,[10] J. Lee,[17] K.B. Lee,[38] K.S. Lee,[32] S Lee,[68] S.H. Lee,[61] M.J. Leitch,[38] M. Leitgab,[24] B. Lewis,[61] X. Li,[11] S.H. Lim,[68] M.X. Liu,[38] D. Lynch,[7] C.F. Maguire,[65] Y.I. Makdisi,[6] M. Makek,[66, 69] A. Manion,[61] V.I. Manko,[33] E. Mannel,[7] T. Maruyama,[28] M. McCumber,[13, 38] P.L. McGaughey,[38] D. McGlinchey,[13, 18] C. McKinney,[24] A. Meles,[49] M. Mendoza,[8] B. Meredith,[14, 24] Y. Miake,[64] T. Mibe,[31] A.C. Mignerey,[40] A.J. Miller,[1] A. Milov,[66] D.K. Mishra,[4] J.T. Mitchell,[7] S. Miyasaka,[55, 63] S. Mizuno,[55, 64] A.K. Mohanty,[4] S. Mohapatra,[60] P. Montuenga,[24] T. Moon,[68] D.P. Morrison,[7, *] M. Moskowitz,[43] T.V. Moukhanova,[33] T. Murakami,[34, 55] J. Murata,[55, 57] A. Mwai,[60] T. Nagae,[34] S. Nagamiya,[31, 55] K. Nagashima,[21] J.L. Nagle,[13, †] M.I. Nagy,[16] I. Nakagawa,[55, 56] H. Nakagomi,[55, 64] Y. Nakamiya,[21] K.R. Nakamura,[34, 55] T. Nakamura,[55] K. Nakano,[55, 63] C. Nattrass,[62] P.K. Netrakanti,[4] M. Nihashi,[21, 55] T. Niida,[64] S. Nishimura,[12, 31] R. Nouicer,[7, 56] T. Novák,[30, 67] N. Novitzky,[29, 61] A.S. Nyanin,[33] E. O'Brien,[7] C.A. Ogilvie,[27] H. Oide,[12] K. Okada,[56] J.D. Orjuela Koop,[13] J.D. Osborn,[42] A. Oskarsson,[39] H. Ozaki,[64] K. Ozawa,[31] R. Pak,[7] V. Pantuev,[25] V. Papavassiliou,[49] I.H. Park,[17] J.S. Park,[59] S. Park,[59] S.K. Park,[32] S.F. Pate,[49] L. Patel,[19] M. Patel,[27] J.-C. Peng,[24] D.V. Perepelitsa,[7, 14] G.D.N. Perera,[49] D.Yu. Peressounko,[33] J. Perry,[27] R. Petti,[7, 61] C. Pinkenburg,[7] R. Pinson,[1] R.P. Pisani,[7] M.L. Purschke,[7] H. Qu,[1] J. Rak,[29] B.J. Ramson,[42] I. Ravinovich,[66] K.F. Read,[51, 62] D. Reynolds,[60] V. Riabov,[47, 54] Y. Riabov,[54, 58] E. Richardson,[40] T. Rinn,[27] N. Riveli,[50] D. Roach,[65] S.D. Rolnick,[8] M. Rosati,[27] Z. Rowan,[5] J.G. Rubin,[42] M.S. Ryu,[20] B. Sahlmueller,[61] N. Saito,[31] T. Sakaguchi,[7] H. Sako,[28] V. Samsonov,[47, 54] M. Sarsour,[19] S. Sato,[28] S. Sawada,[31] B. Schaefer,[65] B.K. Schmoll,[62] K. Sedgwick,[8] J. Seele,[56] R. Seidl,[55, 56] Y. Sekiguchi,[12] A. Sen,[19, 62] R. Seto,[8] P. Sett,[4] A. Sexton,[40] D. Sharma,[61] A. Shaver,[27] I. Shein,[23] T.-A. Shibata,[55, 63] K. Shigaki,[21] M. Shimomura,[27, 46, 64] K. Shoji,[55] P. Shukla,[4] A. Sickles,[7, 24] C.L. Silva,[38] D. Silvermyr,[39, 51] B.K. Singh,[3] C.P. Singh,[3] V. Singh,[3] M. Skolnik,[43] M. Slunečka,[9] M. Snowball,[38] S. Solano,[43] R.A. Soltz,[37] W.E. Sondheim,[38] S.P. Sorensen,[62] I.V. Sourikova,[7] P.W. Stankus,[51] P. Steinberg,[7] E. Stenlund,[39] M. Stepanov,[41, ‡] A. Ster,[67] S.P. Stoll,[7] M.R. Stone,[13] T. Sugitate,[21] A. Sukhanov,[7] T. Sumita,[55] J. Sun,[61] J. Sziklai,[67] A. Takahara,[12] A. Taketani,[55, 56] Y. Tanaka,[45] K. Tanida,[56, 59] M.J. Tannenbaum,[7] S. Tarafdar,[3, 66] A. Taranenko,[47, 60] E. Tennant,[49] R. Tieulent,[19]

A. Timilsina,[27] T. Todoroki,[55, 64] M. Tomášek,[15, 26] H. Torii,[12] C.L. Towell,[1] M. Towell,[1] R. Towell,[1] R.S. Towell,[1] I. Tserruya,[66] H.W. van Hecke,[38] M. Vargyas,[16, 67] E. Vazquez-Zambrano,[14] A. Veicht,[14] J. Velkovska,[65] R. Vértesi,[67] M. Virius,[15] V. Vrba,[15, 26] E. Vznuzdaev,[54] X.R. Wang,[49, 56] D. Watanabe,[21] K. Watanabe,[55, 57] Y. Watanabe,[55, 56] Y.S. Watanabe,[12, 31] F. Wei,[49] S. Whitaker,[27] A.S. White,[42] S. Wolin,[24] C.L. Woody,[7] M. Wysocki,[51] B. Xia,[50] L. Xue,[19] S. Yalcin,[61] Y.L. Yamaguchi,[12, 61] A. Yanovich,[23] S. Yokkaichi,[55, 56] J.H. Yoo,[32] I. Yoon,[59] Z. You,[38] I. Younus,[36, 48] H. Yu,[53] I.E. Yushmanov,[33] W.A. Zajc,[14] A. Zelenski,[6] S. Zhou,[11] and L. Zou[8]

(PHENIX Collaboration)

[1] *Abilene Christian University, Abilene, Texas 79699, USA*
[2] *Department of Physics, Augustana University, Sioux Falls, South Dakota 57197, USA*
[3] *Department of Physics, Banaras Hindu University, Varanasi 221005, India*
[4] *Bhabha Atomic Research Centre, Bombay 400 085, India*
[5] *Baruch College, City University of New York, New York, New York, 10010 USA*
[6] *Collider-Accelerator Department, Brookhaven National Laboratory, Upton, New York 11973-5000, USA*
[7] *Physics Department, Brookhaven National Laboratory, Upton, New York 11973-5000, USA*
[8] *University of California-Riverside, Riverside, California 92521, USA*
[9] *Charles University, Ovocný trh 5, Praha 1, 116 36, Prague, Czech Republic*
[10] *Chonbuk National University, Jeonju, 561-756, Korea*
[11] *Science and Technology on Nuclear Data Laboratory, China Institute of Atomic Energy, Beijing 102413, P. R. China*
[12] *Center for Nuclear Study, Graduate School of Science, University of Tokyo, 7-3-1 Hongo, Bunkyo, Tokyo 113-0033, Japan*
[13] *University of Colorado, Boulder, Colorado 80309, USA*
[14] *Columbia University, New York, New York 10027 and Nevis Laboratories, Irvington, New York 10533, USA*
[15] *Czech Technical University, Zikova 4, 166 36 Prague 6, Czech Republic*
[16] *ELTE, Eötvös Loránd University, H-1117 Budapest, Pázmány P. s. 1/A, Hungary*
[17] *Ewha Womans University, Seoul 120-750, Korea*
[18] *Florida State University, Tallahassee, Florida 32306, USA*
[19] *Georgia State University, Atlanta, Georgia 30303, USA*
[20] *Hanyang University, Seoul 133-792, Korea*
[21] *Hiroshima University, Kagamiyama, Higashi-Hiroshima 739-8526, Japan*
[22] *Department of Physics and Astronomy, Howard University, Washington, DC 20059, USA*
[23] *IHEP Protvino, State Research Center of Russian Federation, Institute for High Energy Physics, Protvino, 142281, Russia*
[24] *University of Illinois at Urbana-Champaign, Urbana, Illinois 61801, USA*
[25] *Institute for Nuclear Research of the Russian Academy of Sciences, prospekt 60-letiya Oktyabrya 7a, Moscow 117312, Russia*
[26] *Institute of Physics, Academy of Sciences of the Czech Republic, Na Slovance 2, 182 21 Prague 8, Czech Republic*
[27] *Iowa State University, Ames, Iowa 50011, USA*
[28] *Advanced Science Research Center, Japan Atomic Energy Agency, 2-4 Shirakata Shirane, Tokai-mura, Naka-gun, Ibaraki-ken 319-1195, Japan*
[29] *Helsinki Institute of Physics and University of Jyväskylä, P.O.Box 35, FI-40014 Jyväskylä, Finland*
[30] *Károly Róberts University College, H-3200 Gyöngyös, Mátraiút 36, Hungary*
[31] *KEK, High Energy Accelerator Research Organization, Tsukuba, Ibaraki 305-0801, Japan*
[32] *Korea University, Seoul, 136-701, Korea*
[33] *National Research Center "Kurchatov Institute", Moscow, 123098 Russia*
[34] *Kyoto University, Kyoto 606-8502, Japan*
[35] *Laboratoire Leprince-Ringuet, Ecole Polytechnique, CNRS-IN2P3, Route de Saclay, F-91128, Palaiseau, France*
[36] *Physics Department, Lahore University of Management Sciences, Lahore 54792, Pakistan*
[37] *Lawrence Livermore National Laboratory, Livermore, California 94550, USA*
[38] *Los Alamos National Laboratory, Los Alamos, New Mexico 87545, USA*
[39] *Department of Physics, Lund University, Box 118, SE-221 00 Lund, Sweden*
[40] *University of Maryland, College Park, Maryland 20742, USA*
[41] *Department of Physics, University of Massachusetts, Amherst, Massachusetts 01003-9337, USA*
[42] *Department of Physics, University of Michigan, Ann Arbor, Michigan 48109-1040, USA*
[43] *Muhlenberg College, Allentown, Pennsylvania 18104-5586, USA*
[44] *Myongji University, Yongin, Kyonggido 449-728, Korea*
[45] *Nagasaki Institute of Applied Science, Nagasaki-shi, Nagasaki 851-0193, Japan*
[46] *Nara Women's University, Kita-uoya Nishi-machi Nara 630-8506, Japan*
[47] *National Research Nuclear University, MEPhI, Moscow Engineering Physics Institute, Moscow, 115409, Russia*
[48] *University of New Mexico, Albuquerque, New Mexico 87131, USA*
[49] *New Mexico State University, Las Cruces, New Mexico 88003, USA*
[50] *Department of Physics and Astronomy, Ohio University, Athens, Ohio 45701, USA*
[51] *Oak Ridge National Laboratory, Oak Ridge, Tennessee 37831, USA*
[52] *IPN-Orsay, Univ. Paris-Sud, CNRS/IN2P3, Université Paris-Saclay, BP1, F-91406, Orsay, France*
[53] *Peking University, Beijing 100871, P. R. China*
[54] *PNPI, Petersburg Nuclear Physics Institute, Gatchina, Leningrad region, 188300, Russia*

[55] *RIKEN Nishina Center for Accelerator-Based Science, Wako, Saitama 351-0198, Japan*
[56] *RIKEN BNL Research Center, Brookhaven National Laboratory, Upton, New York 11973-5000, USA*
[57] *Physics Department, Rikkyo University, 3-34-1 Nishi-Ikebukuro, Toshima, Tokyo 171-8501, Japan*
[58] *Saint Petersburg State Polytechnic University, St. Petersburg, 195251 Russia*
[59] *Department of Physics and Astronomy, Seoul National University, Seoul 151-742, Korea*
[60] *Chemistry Department, Stony Brook University, SUNY, Stony Brook, New York 11794-3400, USA*
[61] *Department of Physics and Astronomy, Stony Brook University, SUNY, Stony Brook, New York 11794-3800, USA*
[62] *University of Tennessee, Knoxville, Tennessee 37996, USA*
[63] *Department of Physics, Tokyo Institute of Technology, Oh-okayama, Meguro, Tokyo 152-8551, Japan*
[64] *Center for Integrated Research in Fundamental Science and Engineering, University of Tsukuba, Tsukuba, Ibaraki 305, Japan*
[65] *Vanderbilt University, Nashville, Tennessee 37235, USA*
[66] *Weizmann Institute, Rehovot 76100, Israel*
[67] *Institute for Particle and Nuclear Physics, Wigner Research Centre for Physics, Hungarian Academy of Sciences (Wigner RCP, RMKI) H-1525 Budapest 114, POBox 49, Budapest, Hungary*
[68] *Yonsei University, IPAP, Seoul 120-749, Korea*
[69] *University of Zagreb, Faculty of Science, Department of Physics, Bijenička 32, HR-10002 Zagreb, Croatia*
(Dated: December 8, 2015)

PHENIX measurements are presented for the cross section and double-helicity asymmetry (A_{LL}) in inclusive π^0 production at midrapidity from $p+p$ collisions at $\sqrt{s} = 510$ GeV from data taken in 2012 and 2013 at the Relativistic Heavy Ion Collider. The next-to-leading-order perturbative-quantum-chromodynamics theory calculation is in excellent agreement with the presented cross section results. The calculation utilized parton-to-pion fragmentation functions from the recent DSS14 global analysis, which prefer a smaller gluon-to-pion fragmentation function. The π^0 A_{LL} results follow an increasingly positive asymmetry trend with p_T and $\sqrt{s}$ with respect to the predictions and are in excellent agreement with the latest global analysis results. This analysis incorporated earlier results on π^0 and jet A_{LL}, and suggested a positive contribution of gluon polarization to the spin of the proton ΔG for the gluon momentum fraction range $x > 0.05$. The data presented here extend to a currently unexplored region, down to $x \sim 0.01$, and thus provide additional constraints on the value of ΔG.

In the late 1980s, the EMC experiment [1] showed that the spins of quarks and anti-quarks might contribute only a fraction of the proton spin (about 1/3 from the recent global analyses of world spin polarized scattering data [2–6]). This sparked several decades of world-wide effort to understand the proton spin structure in terms of quark and gluon polarizations and their orbital angular momentum, as evidenced by experimental programs at CERN, SLAC, DESY, JLAB, and BNL.

A key component of the Relativistic Heavy Ion Collider (RHIC) Spin program is the determination of the gluon spin contribution to the spin of the proton. High energy polarized proton collisions provide direct access to the gluon polarization ΔG within the proton through several gluon dominated hard scattering processes, such as high p_T jet and hadron production [7]. RHIC results on the double helicity asymmetry A_{LL} in inclusive π^0 production at $\sqrt{s} = 62.4$ and 200 GeV from PHENIX [8–11] and jet production at $\sqrt{s} = 200$ GeV from STAR [12, 13] have made a significant contribution to the ΔG determination [2, 3]. Inclusion of the recent RHIC results from $\sqrt{s} = 200$ GeV data collected in 2009 [14, 15] in the global next-to-leading-order (NLO) perturbative-quantum-chromodynamics (pQCD) analysis provided evidence for positive gluon polarization within the proton, with the integral of $\Delta G(x, Q^2 = 10$ GeV$^2)$ in the gluon momentum fraction $x > 0.05$ being $0.20^{+0.06}_{-0.07}$ at 90%

C.L. [16]. The RHIC high luminosity data at $\sqrt{s} = 510$ GeV allow probing ΔG in the overlapping x range at higher momentum transfer, and extends our understanding of ΔG to the unexplored lower x region.

In this Letter, we present the PHENIX π^0 A_{LL} results at $\sqrt{s} = 510$ GeV from the RHIC 2012 and 2013 data sets, with an integrated luminosity of 20 and 108 pb^{-1}, respectively. We also present and discuss our results on π^0 unpolarized cross section measurements, which serve as an important test for the applicability of the NLO pQCD theory calculations in the accessed kinematic range. The theory is used to connect the measured asymmetries to gluon polarization in the proton [2, 3, 16].

The PHENIX experimental setup is described elsewhere [17]. In this analysis, π^0s were reconstructed via $\pi^0 \to \gamma\gamma$ decays using a highly-segmented electromagnetic calorimeter (EMCal), covering a pseudorapidity range of $|\eta| < 0.35$. The EMCal comprises two calorimeter types, a lead-scintillator (PbSc) sampling calorimeter and a lead-glass (PbGl) Čerenkov calorimeter, with granularity $\Delta\eta \times \Delta\phi \sim 0.011 \times 0.011$ and 0.008×0.008, respectively. Eight EMCal sectors (six PbSc and two PbGl) are located in two nearly back-to-back arms each covering $\Delta\phi \sim 90°$ in azimuth. The PHENIX EMCal also generates a high p_T photon (HPP) trigger when the deposited energy in any set of 4×4 towers exceeds a predefined threshold. Thin multiwire proportional cham-

bers located in front of the EMCal were used as a veto to suppress the charged hadron background in π^0 reconstruction [14]. Beam-beam counters (BBC), positioned at ± 144 cm from the nominal interaction point along the beam line and covering $\eta = \pm 3.0$–3.9, defined the minimum-bias (MB) collision trigger and determined the location of the collision vertex. Only events with collision vertices within ± 10 cm (± 30 cm) of the nominal interaction point were used in the cross section (asymmetry) analysis. The BBCs were also used to calculate the integrated luminosity of the collected data sample and relative luminosity between colliding bunches with different spin configurations. Zero-degree calorimeters (ZDC), located at ± 18 m and covering $|\eta| > 6$, were used as another relative luminosity monitor. Equipped with a shower-maximum detector, the ZDC also provided monitoring of the transverse polarization component of colliding bunches in the PHENIX interaction region, utilizing the azimuthal asymmetry in forward neutron production in transversely polarized $p+p$ collisions [18].

As described in detail in Ref. [9], π^0s were reconstructed from two-photon invariant mass distributions. A time of flight cut and shower profile evaluation (energy distribution among EMCal towers) were used for photon identification. A minimal photon energy cut of 0.3 GeV and an energy asymmetry between the two photons $\alpha = |E1 - E2|/(E1 + E2) < 0.8$ were applied. The π^0 peak width in the invariant mass distribution varied between 9 and 12 MeV/c^2 over the measured p_T range. The resulting background fraction in the mass window of ± 25 MeV/c^2 around the π^0 peak varied from $\sim 20\%$ at $p_T \sim 2$ GeV/c to $< 8\%$ at $p_T > 5$ GeV/c. The two decay photons start merging in the PbSc (PbGl) EMCal at π^0 $p_T > 10$ GeV/c (> 15 GeV/c). A 50% merging probability is reached at $p_T \sim 17$ GeV/c (25 GeV/c) in the PbSc (PbGl), as shown in Fig. 1. For $p_T > 24$ GeV/c, the majority of photon pairs are merged in the PbSc; in this p_T range, only the PbGl data were used.
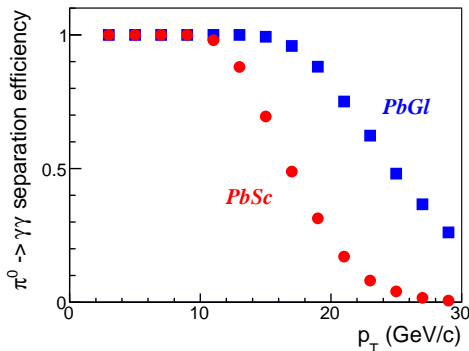

FIG. 1. (color online) The probability for two photons from π^0 decay to be separated by the PHENIX EMCal clustering algorithm vs π^0 p_T; obtained from GEANT [19] simulation for the two-photon energy asymmetry cut $\alpha < 0.8$.

The invariant differential cross section for π^0 production is calculated as

$$E\frac{d^3\sigma}{dp^3} = \frac{1}{\mathcal{L}} \cdot \frac{1}{2\pi p_T^*} \cdot \frac{C \cdot N}{\Delta p_T \Delta y}, \qquad (1)$$

where N is the number of π^0's observed in a Δp_T wide bin at p_T^* defined as the p_T for which the cross section equals its average over the bin; Δy is the rapidity range; C includes corrections for trigger efficiency, geometrical acceptance, π^0 reconstruction efficiency, and detector resolution effects; $\mathcal{L}$ is the integrated luminosity for the analyzed data sample.

Two data samples were used for the π^0 cross section measurements, one collected with a MB trigger and the other with the HPP in coincidence with MB trigger. The MB trigger efficiency was obtained from the data collected with a dedicated HPP trigger operated without coincidence with MB trigger, and found to be 0.91 ± 0.01 independent of p_T. It accounts for the fact that only a fraction of inelastic $p+p$ collisions producing π^0 meson(s) fires the MB trigger. The HPP trigger efficiency vs p_T was calculated in each arm separately from a set of events triggered by a high energy cluster in the opposite arm. It showed a characteristic threshold behavior with efficiency increasing from $\sim 1\%$ at $p_T = 2$ GeV/c to 93% at $p_T > 8$ GeV/c. For the cross section calculation, the MB triggered data sample was used at $p_T < 6$ GeV/c, and HPP triggered data sample at higher p_T.

The reconstructed π^0 yields in each p_T bin were corrected for geometrical acceptance, reconstruction efficiencies (e.g. due to the two-photon energy asymmetry cut), and smearing effects (due to the finite detector resolutions). The corrections were calculated with a simulation containing the EMCal geometry, known detector inefficiencies, and photon energy and position smearing based on the known EMCal resolutions.

The major systematic uncertainties in the π^0 cross section measurement are the energy scale (1.2% uncertainty in the EMCal energy calibration translates to $\sim 7\%$ in cross section uncertainty), energy nonlinearity (up to 10% for cross section depending on p_T), and merging corrections (up to 30% in the bins with the highest probability for two photons to merge). The large uncertainty at high p_T reflects the sensitivity of the merging correction to shower-shape fluctuations and background conditions for asymmetric two-photon decays, having higher probability to survive the merging in the EMCal. The other uncertainties, contributing $< 6\%$ altogether, are related to π^0 yield extraction and background subtraction, trigger efficiencies, geometrical acceptance calculation, smearing corrections, and photon conversion. The uncertainties are assigned separately for the PbSc and the PbGl measurements.

A comparison of the results obtained from the PbSc and the PbGl is a key cross check, because the two calorimeters have a different response to hadrons (hence

different background contamination in π^0 reconstruction), and considerably different merging corrections versus p_T. The π^0 cross section results from the PbSc and the PbGl were in agreement within uncertainties in the overlapping p_T range. The final spectrum was obtained from the combined PbSc and PbGl results, while for $p_T > 24$ GeV/c the PbGl results were used. The total systematic uncertainties associated with the results vary from 8–10% at $p_T < 14$ GeV/c to $\sim$30% at the highest p_T.

The integrated luminosity $\mathcal{L}$ in Eq.(1) was calculated from the accumulated number of MB triggers in the analyzed data sample normalized by the cross section of the processes firing the MB trigger in $p+p$ collisions. Similar to our previous analyses [10, 20], the cross section was defined using a vernier scan technique and found to be 32.5 mb with $\pm$10% uncertainty.

In the 2013 RHIC run, the instantaneous luminosity delivered to PHENIX was so high that up to a third of all bunch crossings had more than one $p+p$ collision. To correct for this multiple-collision effect, we studied the ratio of the π^0 yield to the number of MB triggers (which is proportional to the measured $N/\mathcal{L}$ in Eq.(1)) as a function of instantaneous MB trigger rate.

Figure 2 shows the π^0 cross section versus p_T compared to NLO pQCD calculations performed with MSTW [21] parton distribution functions (PDF) and DSS14 [22] fragmentation functions (FF). Compared to earlier FF analysis [23] the DSS14 recent global fit results preferred a smaller fraction of pions produced from gluon hadronization, driven mainly by the latest data from the Large Hadron Collider. This theoretical calculation is in excellent agreement with the presented data.

In 2012 and 2013, RHIC provided PHENIX with colliding bunches of longitudinally polarized protons at $\sqrt{s} = $ 510 GeV. The bunch spin pattern was predefined in such a way that the colliding bunch pair helicity state alternated every bunch crossing, spaced 106 ns apart. This greatly suppressed the possibility of false asymmetries between colliding bunches with different helicity configuration, due to variation in detector performance. To remove possible systematic effects associated with particular bunch(es) in the process of filling, ramping up and storing the beams in RHIC rings, eight bunch spin patterns were used alternating every RHIC store, typically lasting eight hours. Beam polarizations were measured by RHIC polarimeters [24] three-to-four times during the store. For the two RHIC collider rings, labeled "Blue" (B) and "Yellow" (Y), the luminosity-weighted average polarizations in 2012 (2013) were $\langle P_B \rangle = 0.55 \pm 0.02$ (0.55 ± 0.02) and $\langle P_Y \rangle = 0.57 \pm 0.02$ (0.56 ± 0.02). The degree of longitudinal polarization in the PHENIX interaction region was monitored by local polarimeters, based on the ZDC and shower-maximum detectors, which measured the residual transverse polarization of colliding bunches. The longitudinal component P_L/P in both
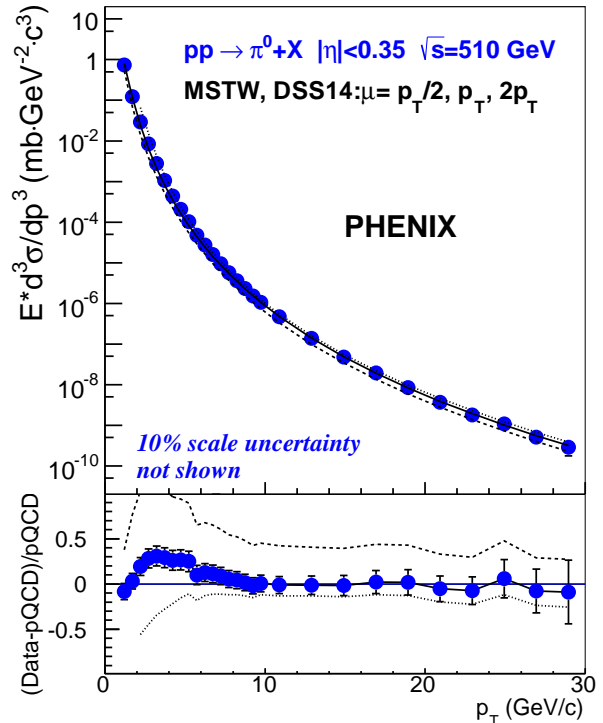

FIG. 2. (color online) The neutral pion production cross section at midrapidity in $p+p$ collisions at $\sqrt{s} = 510$ GeV as a function of p_T and NLO pQCD calculations for theory scales $\mu = p_T/2$ (dotted line), p_T (solid line) and $2p_T$ (dashed line), with μ representing equal factorization, renormalization, and fragmentation scales. Note that the error bars, representing the combined statistical and point-to-point systematic uncertainties, are smaller than the points. (bottom panel) Relative difference between the data and theory for the three theory scales. Experimental uncertainties are shown for the $\mu = p_T$ curve.

2012 and 2013 was > 0.998, for both RHIC rings.

The π^0 A_{LL} analysis technique is described in detail in Ref. [14]. The A_{LL} for inclusive π^0 production, defined as the difference between cross sections for colliding bunches with the same helicity and opposite helicity, divided by the sum, is experimentally calculated as

$$A_{LL}^{\pi^0} = \frac{1}{P_B \cdot P_Y} \cdot \frac{N_{++} - R \cdot N_{+-}}{N_{++} + R \cdot N_{+-}}; \quad R = \frac{L_{++}}{L_{+-}}, \quad (2)$$

where N is the number of π^0's from the colliding bunches with the same $(++)$ and opposite $(+-)$ helicities, R is the relative luminosity between bunches with the same and opposite helicities, and P_B and P_Y are the two RHIC beam polarizations.

The π^0 yields were extracted from the HPP triggered sample in which the maximal energy photon of each pair candidate was explicitly required to fire the HPP trigger. This test, along with a time-of-flight cut, suppressed the

possibility of contamination from the neighboring bunch crossings to a negligible level. As in the cross section analysis, the π^0 candidates were counted within a ± 25 MeV/c^2 window around the π^0 peak in the two-photon invariant mass distribution. The A_{LL} was then corrected for the background A_{LL} measured in the side bands on either side of the π^0 peak; this background asymmetry was found to be consistent with zero in all p_T bins.

The relative luminosity R was defined from the number of MB triggers in each bunch crossing, and cross checked using the number of collisions firing the ZDCs on both sides of the IR. The pile-up correction due to the high collision rate had a negligible effect on R. The resulting contribution of the relative luminosity uncertainty to $A_{LL}^{\pi^0}$ for the 2012 (2013) data was $\delta A_{LL}^{\pi^0}|_R = 2.0 \times 10^{-4}$ (3.8×10^{-4}), affecting all p_T bins in the same way.

A_{LL} was measured for each PHENIX data taking segment (up to 90 minutes long) to minimize the systematic effects from variation in R, beam polarization (decreasing during a store by ΔP=0.005–0.010 per hour), and HPP trigger performance. These asymmetries were averaged separately for the 2012 and 2013 data. Results from 2012 and 2013 were consistent within statistical uncertainties and the final result presented in this Letter is the average of these data sets.

The resulting π^0 A_{LL} systematic uncertainties are (a) a correlated uncertainty from relative luminosity of 3.6×10^{-4}, (b) a correlated uncertainty from polarization measurements of 6.5% (scale uncertainty), and (c) point-to-point uncertainty from background fraction determination under the π^0 peak in the two-photon invariant-mass distribution. The point-to-point uncertainties were found to be smaller than 10% of the statistical uncertainty in all p_T bins. As in the previous PHENIX analysis [14], the contribution of other potential sources of systematic uncertainties was negligible.

Figure 3 shows the π^0 A_{LL} asymmetries at $\sqrt{s} = 510$ GeV compared with the DSSV14 calculation [16] based on a global fit of the world helicity asymmetry data. Comparing the data to the DSSV14 curve we obtain χ^2/NDF=8.0/14, while comparing to the $A_{LL} = 0$ hypothesis we obtain χ^2/NDF = 18.2/14; the data prefer the DSSV14 curve by a little more than 3 standard deviations.

Figure 4 shows π^0 A_{LL} data from PHENIX at both $\sqrt{s} = 200$ GeV [14] and 510 GeV, along with NLO pQCD analyses from three groups [5, 6, 16]. All three analyses predict an increase in π^0 A_{LL} at the same x_T due to pQCD evolution, with $x_T = 2p_T/\sqrt{s}$. Our data is consistent with such an increase.

In summary, we have presented the unpolarized cross section and double helicity asymmetry for π^0 production at midrapidity for $p+p$ collisions at $\sqrt{s} = 510$ GeV. The NLO pQCD calculation is in excellent agreement with the presented cross section results. The calculation utilized the recent DSS14 set of fragmentation functions,
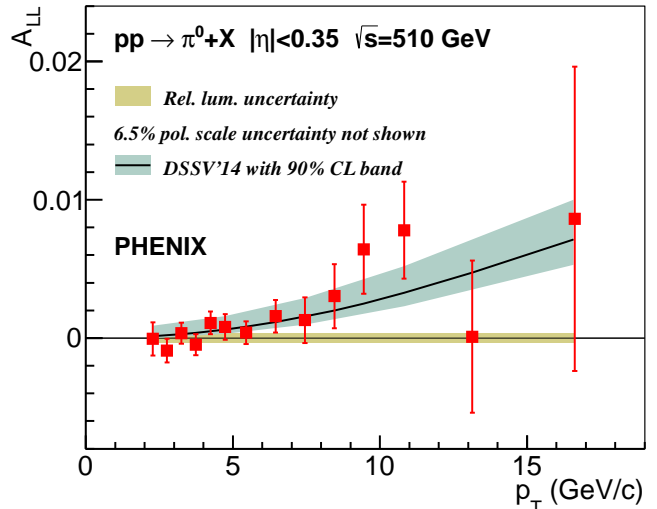

FIG. 3. (color online) A_{LL} vs p_T for π^0 production at midrapidity in $p+p$ collisions at $\sqrt{s} = 510$ GeV. Error bars are combined statistical and point-to-point systematic uncertainties. The $A_{LL} = 0$ (yellow) line is uncertainty from relative luminosity. The theoretical curve with 90% C.L. band (green) is from a DSSV14 calculation [16].
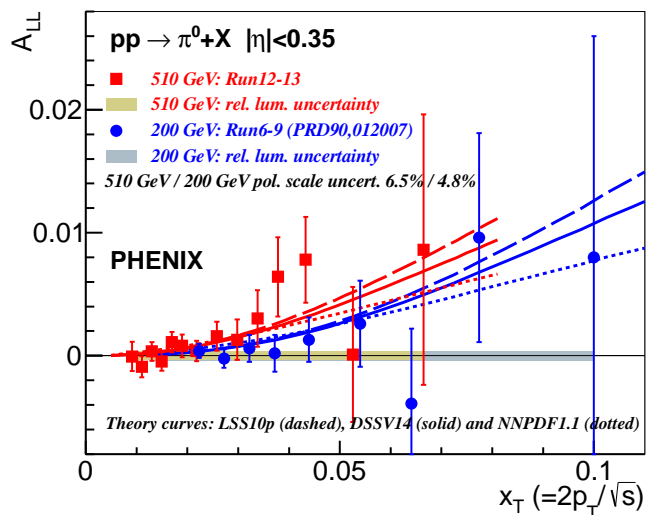

FIG. 4. (color online) A_{LL} vs x_T for π^0 production at midrapidity at $\sqrt{s} = 200$ GeV (blue) from [14] and 510 GeV (red) from this analysis. Error bars are combined statistical and point-to-point systematic uncertainties. Note that the relative luminosity uncertainties from two data samples are about the same, hence are indistinguishable in the plot in the overlapping x_T range. Theoretical curves are from recent NLO global analyses [5, 6, 16], with the lower curves (blue) for $\sqrt{s} = 200$ GeV and the higher curves (red) for $\sqrt{s} = 510$ GeV.

which prefer the reduced fraction of pions produced from gluon hadronization. The π^0 A_{LL} results follow a positive asymmetry trend with p_T and $\sqrt{s}$ predicted by NLO pQCD and are in excellent agreement with the latest global fit results, which suggested a nonzero gluon polarization in the proton for the gluon momentum fraction range $x > 0.05$. These global fit results included RHIC π^0 A_{LL} data at $\sqrt{s} = 62.4$ GeV and 200 GeV and jet A_{LL} data at $\sqrt{s} = 200$ GeV. The presented data at $\sqrt{s} = 510$ GeV extend the x range probed down to $x \sim 0.01$ and provide an additional constraint on ΔG in this x range [25], which is a crucial step in the nearly two decades of world-wide efforts to understand the contribution of gluon polarization to the spin of the proton. We note the recent π^0 A_{LL} results at $\sqrt{s} = 200$ GeV and forward pseudorapidity $0.8 < \eta < 2$ from STAR covering the gluon x range down to $x \sim 0.01$ (although with large uncertainties) [26]. Data collected by PHENIX with forward EMCal at pseudorapidity $3.1 < \eta < 3.9$ and $\sqrt{s} = 510$ GeV will further extend the x range probed down to $x \sim 0.001$.

---

* PHENIX Co-Spokesperson: morrison@bnl.gov
† PHENIX Co-Spokesperson: jamie.nagle@colorado.edu
‡ Deceased

[1] J. Ashman *et al.* (European Muon Collaboration), "An Investigation of the Spin Structure of the Proton in Deep Inelastic Scattering of Polarized Muons on Polarized Protons," Nucl. Phys. B **328**, 1 (1989).

[2] D. de Florian, R. Sassot, M. Stratmann, and W. Vogelsang, "Global Analysis of Helicity Parton Densities and Their Uncertainties," Phys. Rev. Lett. **101**, 072001 (2008).

[3] D. de Florian, R. Sassot, M. Stratmann, and W. Vogelsang, "Extraction of Spin-Dependent Parton Densities and Their Uncertainties," Phys. Rev. D **80**, 034030 (2009).

[4] Johannes Blumlein and Helmut Bottcher, "QCD Analysis of Polarized Deep Inelastic Scattering Data," Nucl. Phys. B **841**, 205 (2010).

[5] E. Leader, A. V. Sidorov, and Dimiter B. Stamenov, "Determination of Polarized PDFs from a QCD Analysis of Inclusive and Semi-inclusive Deep Inelastic Scattering Data," Phys. Rev. D **82**, 114018 (2010).

[6] Richard D. Ball *et al.* (NNPDF Collaboration), "Unbiased determination of polarized parton distributions and their uncertainties," Nucl. Phys. B **874**, 36 (2013).

[7] Gerry Bunce, Naohito Saito, Jacques Soffer, and Werner Vogelsang, "Prospects for spin physics at RHIC," Ann. Rev. Nucl. Part. Sci. **50**, 525 (2000).

[8] S. S. Adler *et al.* (PHENIX Collaboration), "Improved measurement of double helicity asymmetry in inclusive midrapidity pi0 production for polarized p+p collisions at $\sqrt{s} = 200$ GeV," Phys. Rev. D **73**, 091102 (2006).

[9] A. Adare *et al.* (PHENIX Collaboration), "Inclusive cross-section and double helicity asymmetry for pi0 production in p + p collisions at $\sqrt{s} = 200$ GeV: Implications for the polarized gluon distribution in the proton," Phys. Rev. D **76**, 051106 (2007).

[10] A. Adare *et al.* (PHENIX Collaboration), "Inclusive cross section and double helicity asymmetry for π^0 production in $p+p$ collisions at $\sqrt{s} = 62.4$ GeV," Phys. Rev. D **79**, 012003 (2009).

[11] A. Adare *et al.* (PHENIX Collaboration), "The Polarized gluon contribution to the proton spin from the double helicity asymmetry in inclusive π^0 production in polarized $p+p$ collisions at $\sqrt{s} = 200$ GeV," Phys. Rev. Lett. **103**, 012003 (2009).

[12] B. I. Abelev *et al.* (STAR Collaboration), "Longitudinal double-spin asymmetry and cross section for inclusive jet production in polarized proton collisions at $\sqrt{s} = 200$ GeV," Phys. Rev. Lett. **97**, 252001 (2006).

[13] B. I. Abelev *et al.* (STAR Collaboration), "Longitudinal double-spin asymmetry for inclusive jet production in p+p collisions at $\sqrt{s} = 200$ GeV," Phys. Rev. Lett. **100**, 232003 (2008).

[14] A. Adare *et al.* (PHENIX Collaboration), "Inclusive

double-helicity asymmetries in neutral-pion and eta-meson production in $\vec{p} + \vec{p}$ collisions at $\sqrt{s} = 200$ GeV," Phys. Rev. D **90**, 012007 (2014).

[15] L. Adamczyk *et al.* (STAR Collaboration), "Precision Measurement of the Longitudinal Double-spin Asymmetry for Inclusive Jet Production in Polarized Proton Collisions at $\sqrt{s}$ = 200 GeV," Phys. Rev. Lett. **115**, 092002 (2015).

[16] D. de Florian, R. Sassot, M. Stratmann, and W. Vogelsang, "Evidence for polarization of gluons in the proton," Phys. Rev. Lett. **113**, 012001 (2014).

[17] K. Adcox *et al.* (PHENIX Collaboration), "PHENIX detector overview," Nucl. Instrum. Methods Phys. Res., Sec. A **499**, 469 (2003).

[18] A. Adare *et al.* (PHENIX Collaboration), "Inclusive cross section and single transverse spin asymmetry for very forward neutron production in polarized $p+p$ collisions at $\sqrt{s} = 200$ GeV," Phys. Rev. D **88**, 032006 (2013).

[19] GEANT 3.2.1 Manual, CERN, Geneva (1993).

[20] S. S. Adler *et al.* (PHENIX Collaboration), "Mid-rapidity neutral pion production in proton proton collisions at $\sqrt{s}$ = 200 GeV," Phys. Rev. Lett. **91**, 241803 (2003).

[21] A. D. Martin, W. J. Stirling, R. S. Thorne, and G. Watt, "Parton distributions for the LHC," Eur. Phys. J. C **63**, 189 (2009).

[22] D. de Florian, R. Sassot, M. Epele, R. J. Hernandez-Pinto, and M. Stratmann, "Parton-to-Pion Fragmentation Reloaded," Phys. Rev. D **91**, 014035 (2015).

[23] D. de Florian, R. Sassot, and M. Stratmann, "Global analysis of fragmentation functions for protons and charged hadrons," Phys. Rev. D **76**, 074033 (2007).

[24] B. Schmidke *et al.* (RHIC Polarimetry Group), "Run-13 Polarimetry Measurements," RHIC/CAD Accelerator Physics Note 490 (2013).

[25] R. Sassot (DSSV Group), private communication.

[26] L. Adamczyk *et al.* (STAR Collaboration), "Neutral pion cross section and spin asymmetries at intermediate pseudorapidity in polarized proton collisions at $\sqrt{s}$ = 200 GeV," Phys. Rev. D **89**, 012001 (2014).